[60]Fullerene Metal Complexes with Large Effective Two-photon Absorption Cross-section

Fangfang Jian,[1,2] Jing Wang,[2] Hailian Xiao,[2] Pusu Zhao[2], Pingping Sun[2], Lihua Huang[2]*

[1]Microscale Science Institute, Weifang Colledge, Weifang 261061, P. R. China.
[2]New Materials & Function Coordination Chemistry Lab., Qingdao University of Science & Technology Qingdao, 266042, P.R. China.

E-mail: wj_crystal@qust.edu.cn

Supporting information

Table of contents **Page**

1. Crystal Analyst for $\{[(EtO)_2PS_2]_2Ni\}\cdot 2C_{60}$ 2d and $\{[(EtO)_2PS_2]_2Pd\}\cdot 2C_{60}$ 2g

Crystallographic Data Collection. The diffraction data were collected on an Enraf-Nonius CAD4 diffractometer with graphite monchromatic Mo-K_α (λ = 0.71073 Å, T = 293K) radiation. Empirical absorption correction was carried out by using the SADABS program. Their structures were solved by direct methods and refined by least squares on F_{obs}^2 with SHELXTL software package. All non-H atoms were anisotropically refined. The hydrogen atoms were located by difference synthesis and refined isotropically. The molecular graphics were plotted using SHELXTL. Atomic scattering factors and anomalous dispersion corrections were taken from *International Tables for X-ray Crystallography*. A summary of the key crystallographic information for **2d** and **2g** was given in Table S1. Due to many disorder atoms, the structure refinement has not properly converged.

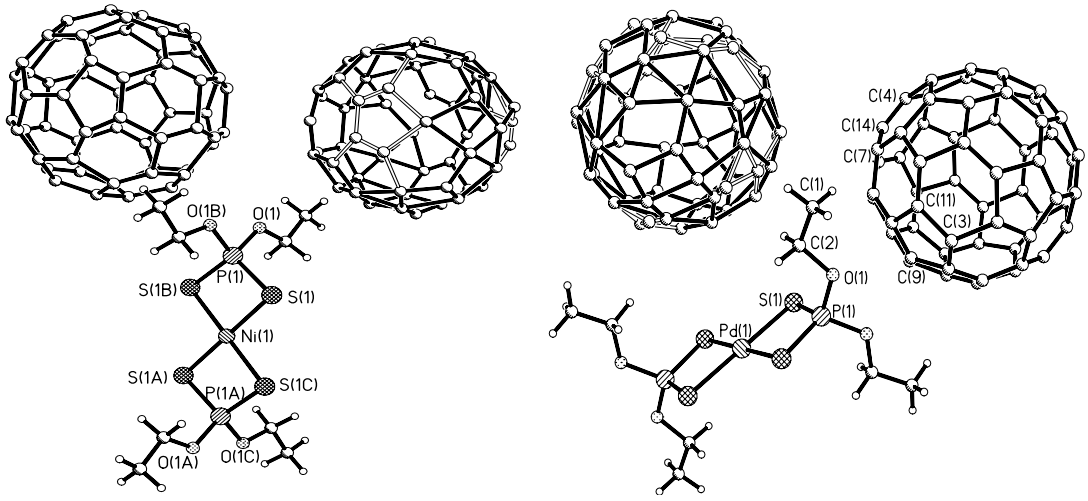

Fig. S0 ORTEP diagram with ellipsoids drawn at 50% probability for 2d $\{[(EtO)_2PS_2]_2Ni\}\cdot 2C_{60}$ [Left] and for 2g $\{[(EtO)_2PS_2]_2Pd\}\cdot 2C_{60}$ [Right].

Table S1 A summary of the key crystallographic information for **2d** and **2g**

	$[(EtO)_2PS_2]_2Ni{\cdot}2C_{60}$ (2d)	**$[(EtO)_2PS_2]_2Pd{\cdot}2C_{60}$ (2g)**
Empirical formula	$C_{128}H_{20}NiO_4P_2S_4$	$C_{128}H_{20}O_4P_2PdS_4$
Formula weight	1870.33	1918.02
T(K)	293(2)	293(2)
Wavelength (Å)	0.71073	0.71073
Crystal system	Monoclinic	Monoclinic
Space group	*C2/m*	*C2/m*
a (Å)	31.509 (6)	31.488(8)
b (Å)	16.407(3)	16.491(3)
c (Å)	10.668(2)	10.072(2)
beta, deg	108.64(3)	108.62(3)
V ($Å^3$)	5225.7(17)	4956.3(18)
Z	2	2
Dc (Mg/m^3)	1.189	1.285
Absorption coefficient (mm^{-1})	0.350	0.360
F(000)	1884	1920
Theta range for data collection (°)	1.42 to 24.49	1.36 to 26.97
Limiting indices	$-34 \le h \le 36$	$-38 \le h \le 40$
	$-19 \le k \le 19$	$-20 \le k \le 20$
	$-11 \le l \le 0$	$-12 \le l \le 0$
Reflections collected / unique	9119/ 4471 [$R_{(int)} = 0.1844$]	11370/5594 [$R_{(int)} = 0.1107$]
Completeness to theta	99.0%	100%
Data / restraints / parameters	4471 / 0 / 449	5594 / 0 / 442
GOF	0.957	1.158
Final R indices [I>2σ(I)]	$R_1 = 0.0912$, $wR_2 = 0.2060$	$R_1 = 0.0869$, $wR_2 = 0.2220$
R indices (all data)	$R_1 = 0.2659$, $wR_2 = 0.2963$	$R_1 = 0.1609$, $wR_2 = 0.2564$
Largest diff. peak and hole($e.Å^{-3}$)	0.480 and -0.823	0.796 and -0.922
Refinement method	Full-matrix least-squares on F^2	

A

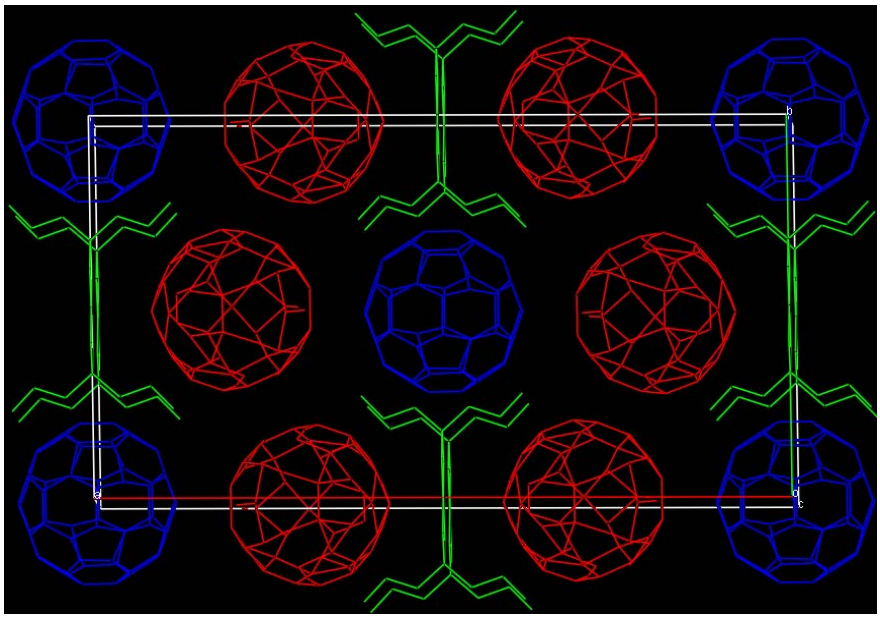

B

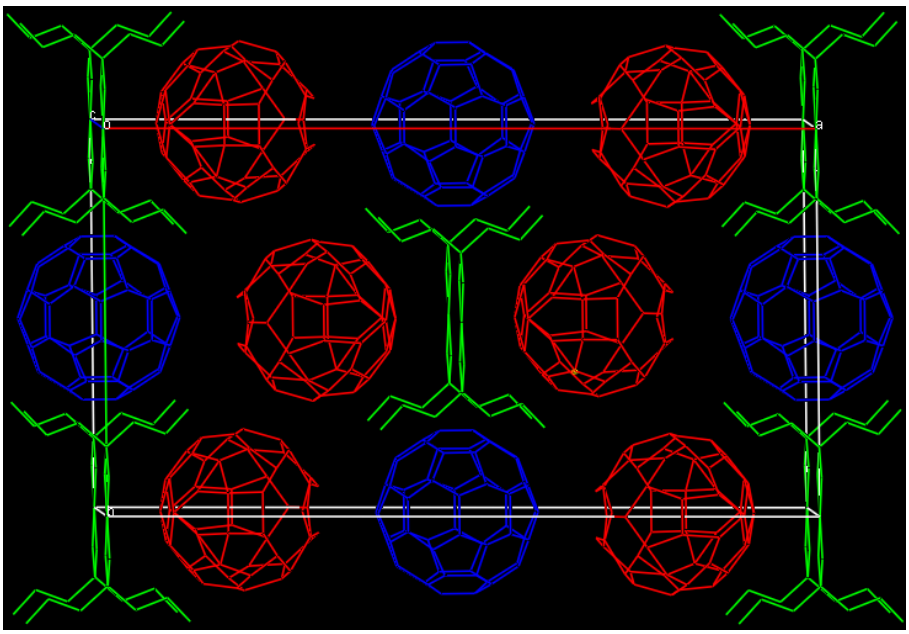

Fig. S1. The view of crystal packing along the c axis; **A**) **2d** $\{[(EtO)_2PS_2]_2Ni\}\cdot 2C_{60}$; **B**) **2g** $\{[(EtO)_2PS_2]_2Pd\}\cdot 2C_{60}$

A

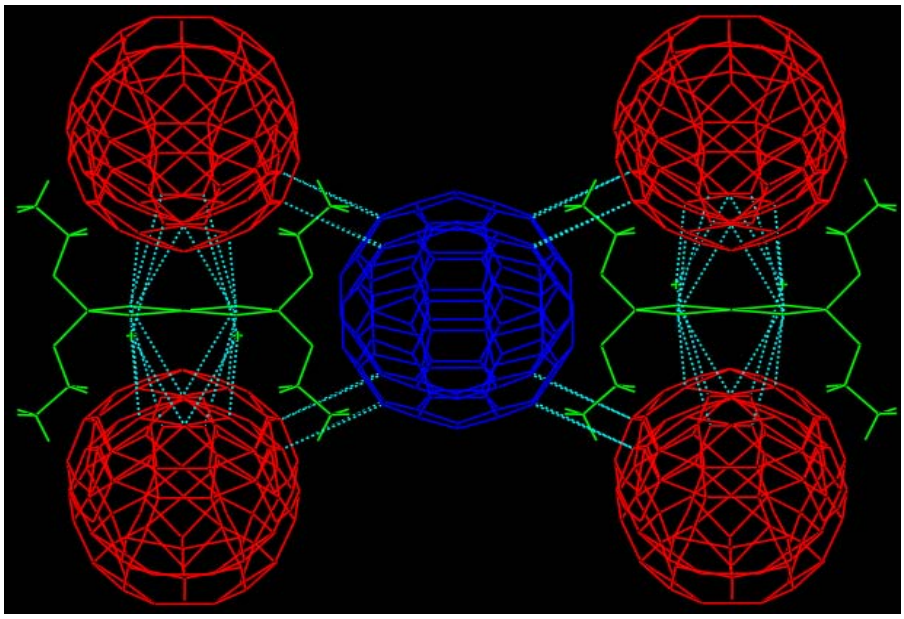

B

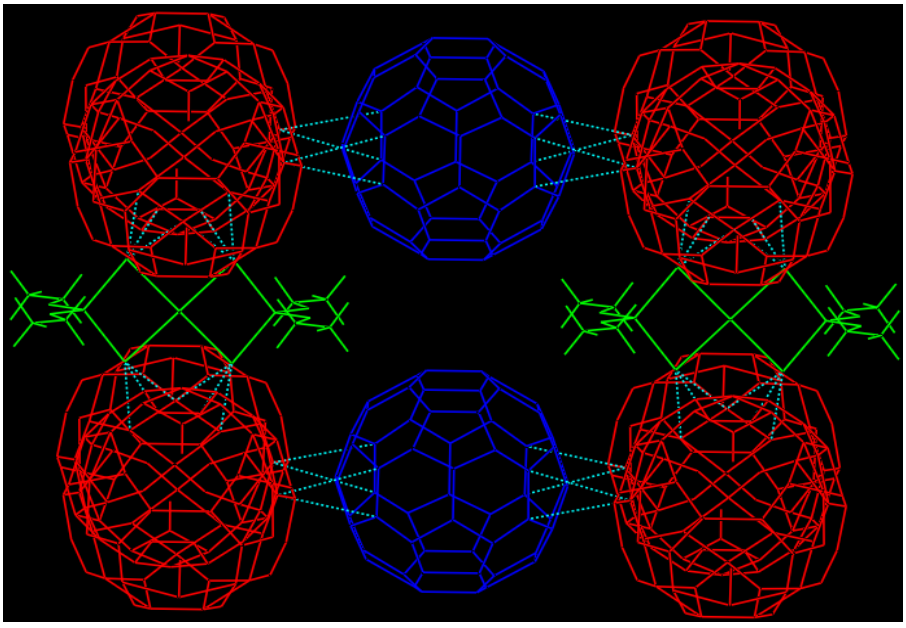

Fig. S2. Van der Waals contacts in the crystal structures of **2d** and **2g**; **A**) along the c axis; **B**) along *a* axis

2. UV-vis spectra

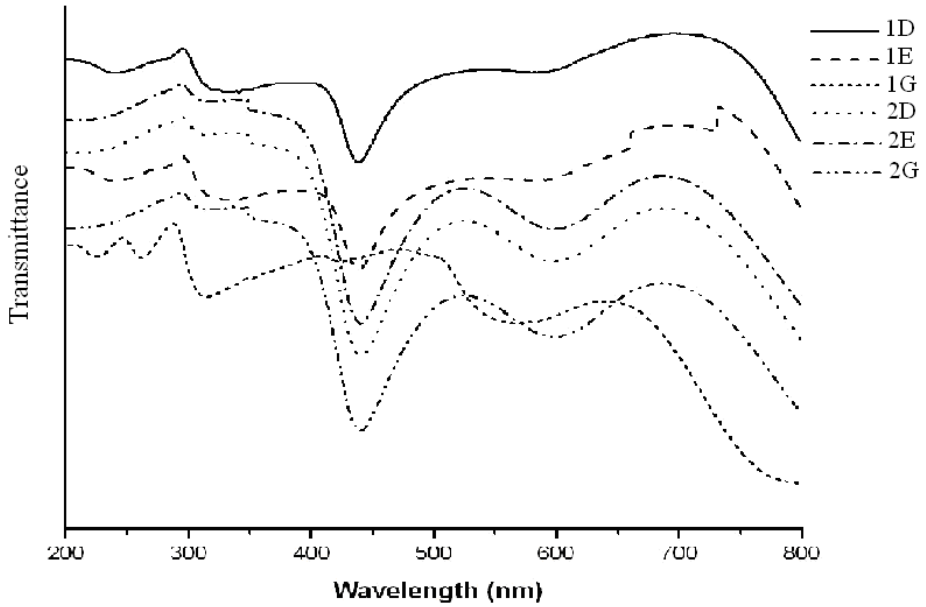

Fig. S3-1 Solid UV-vis spectra of metal dialkyldithiophosphate complexes: 1D, $[(MeO)_2PS_2]_2Ni$; **1E**, $[(MeO)_2PS_2]_2Cu$; **1G,** $[(MeO)_2PS_2]_2Pd$; **2D,** $[(EtO)_2PS_2]_2Ni$; **2E**, $[(EtO)_2PS_2]_2Cu$; **2G,** $[(EtO)_2PS_2]_2Pd$;

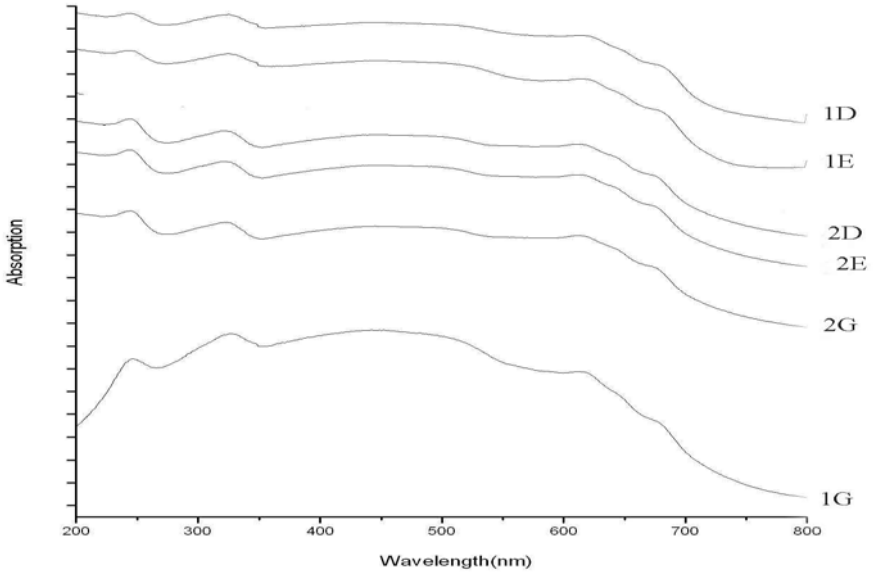

Fig. S3-2 Solid UV-vis spectra of metal fullerene complexes for 1d, 1e, 1g, 2d, 2e and 2g.

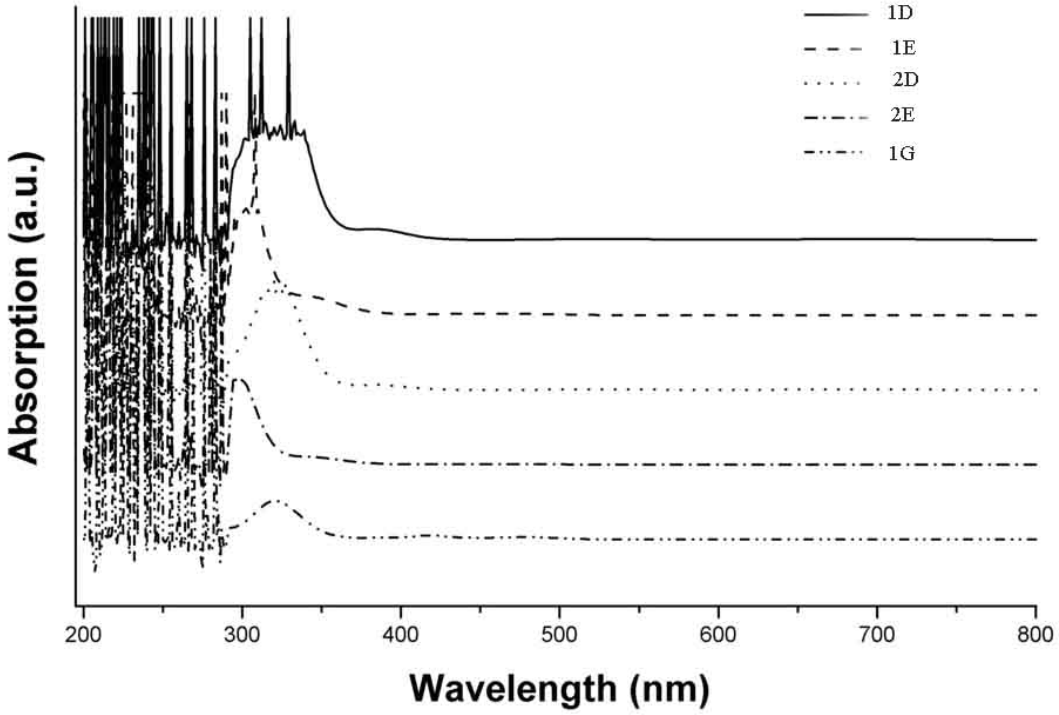

Fig. S3-3 UV-vis spectra of metal dialkyldithiophosphate complexes in *o*-dichlorobenzene: 1D, $[(MeO)_2PS_2]_2Ni$; **1E**,$[(MeO)_2PS_2]_2Cu$; **1G**, $[(MeO)_2PS_2]_2Pd$; **2D**, $[(EtO)_2PS_2]_2Ni$; **2G**, $[(EtO)_2PS_2]_2Pd$;

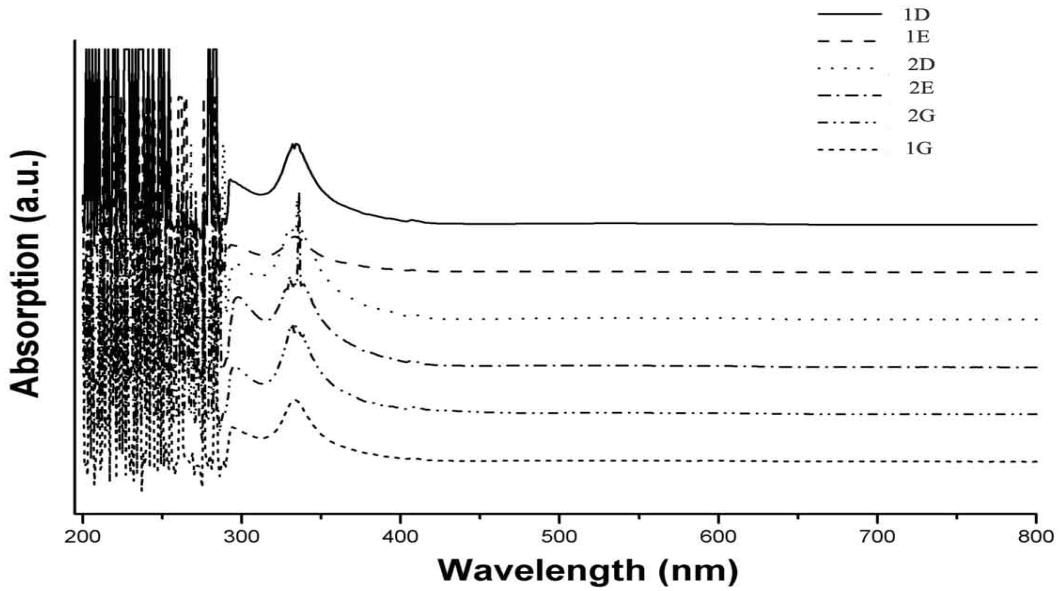

Fig. S3-4 UV-vis spectra of metal fullerene complexes in *o*-dichlorobenzene for 1d, 1e, 1g, 2d, 2e and 2g.

3. IR spectra

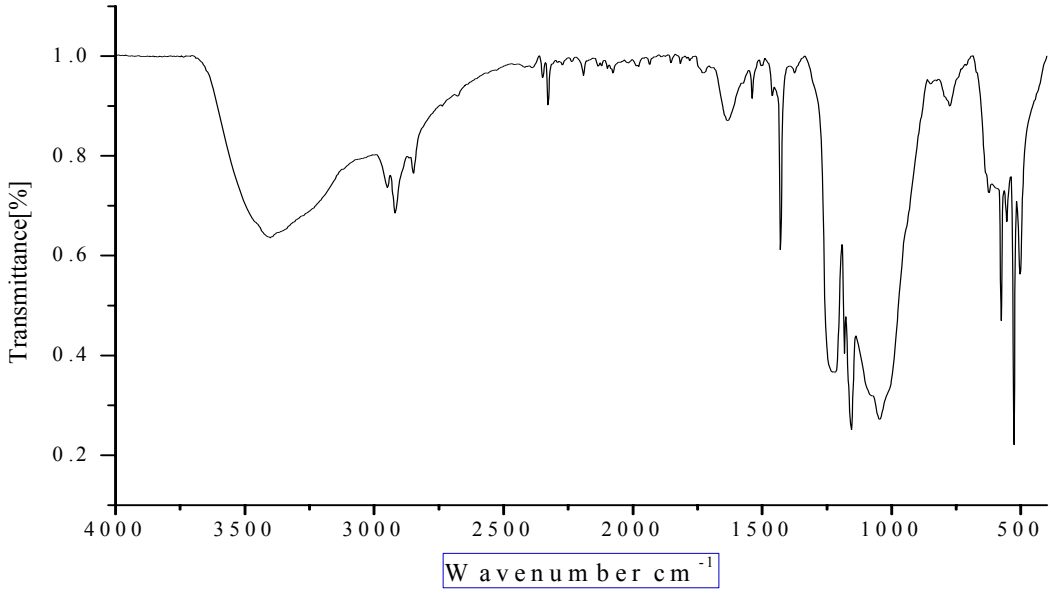

Fig. S4-1 The IR spectra of 1a

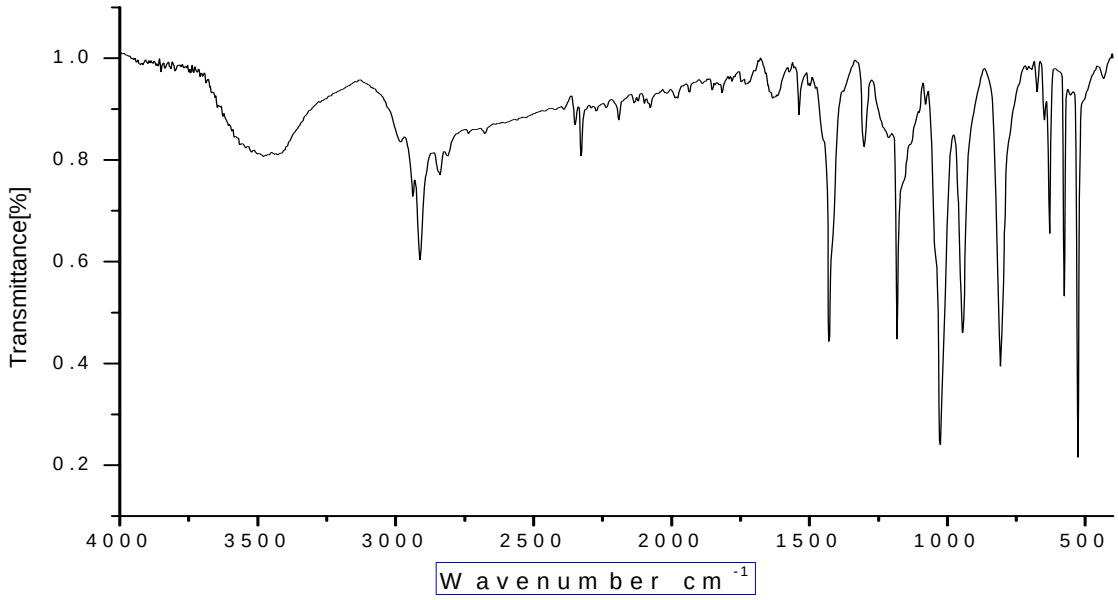

Fig. S4-2 The IR spectra of 1b

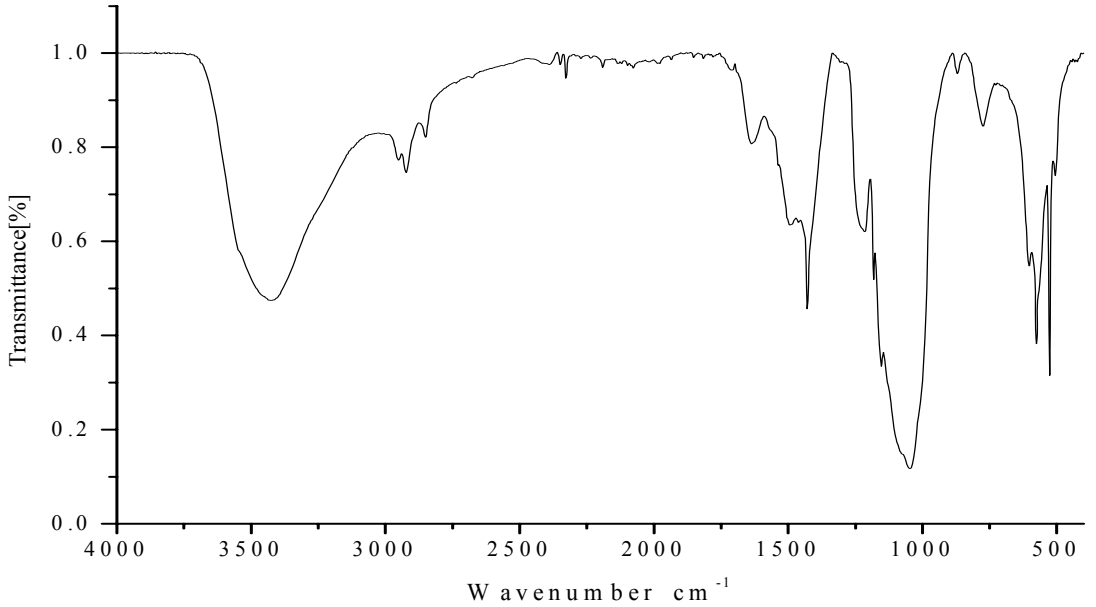

Fig. S4-3 The IR spectra of 1c

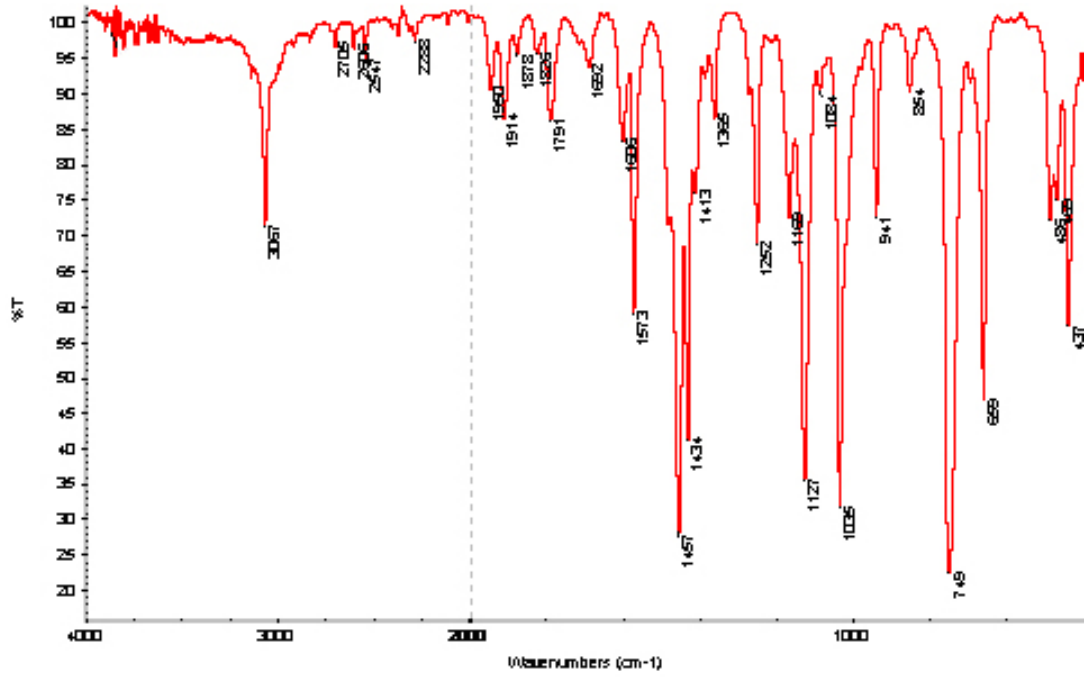

Fig. S4-4 The IR spectra of 1d

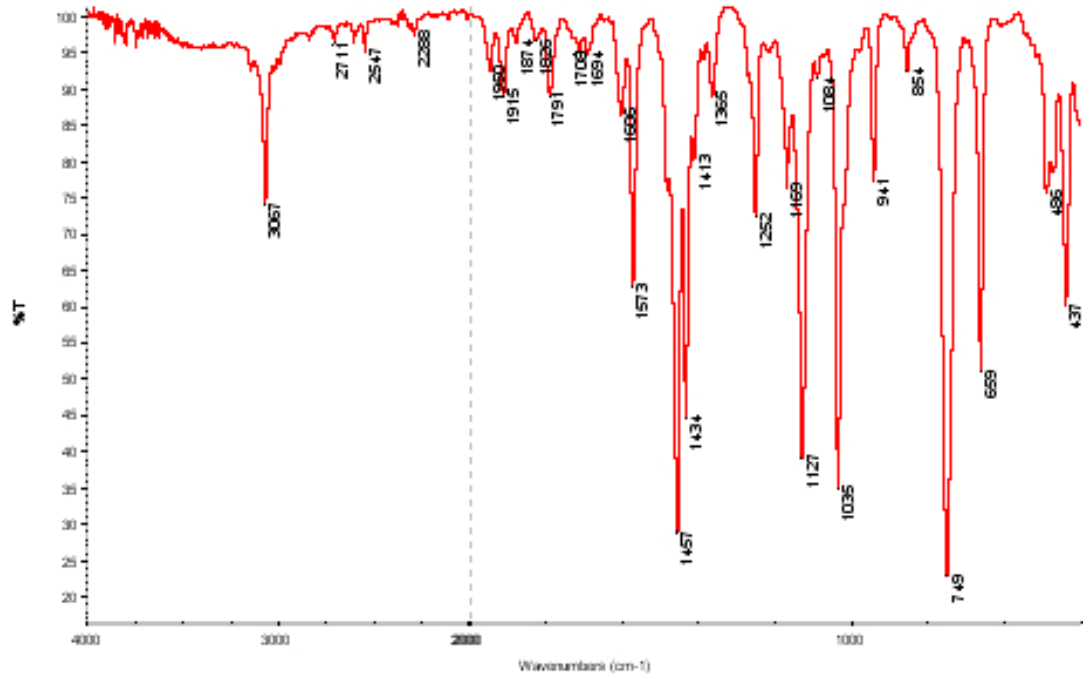

Fig. S4-5 The IR spectra of 1e

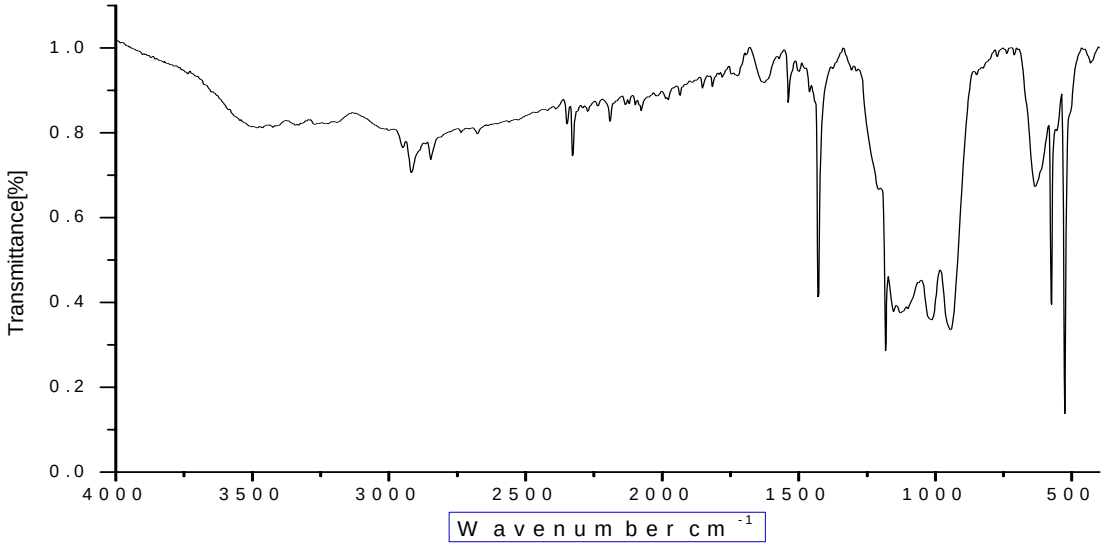

Fig. S4-6 The IR spectra of 1f

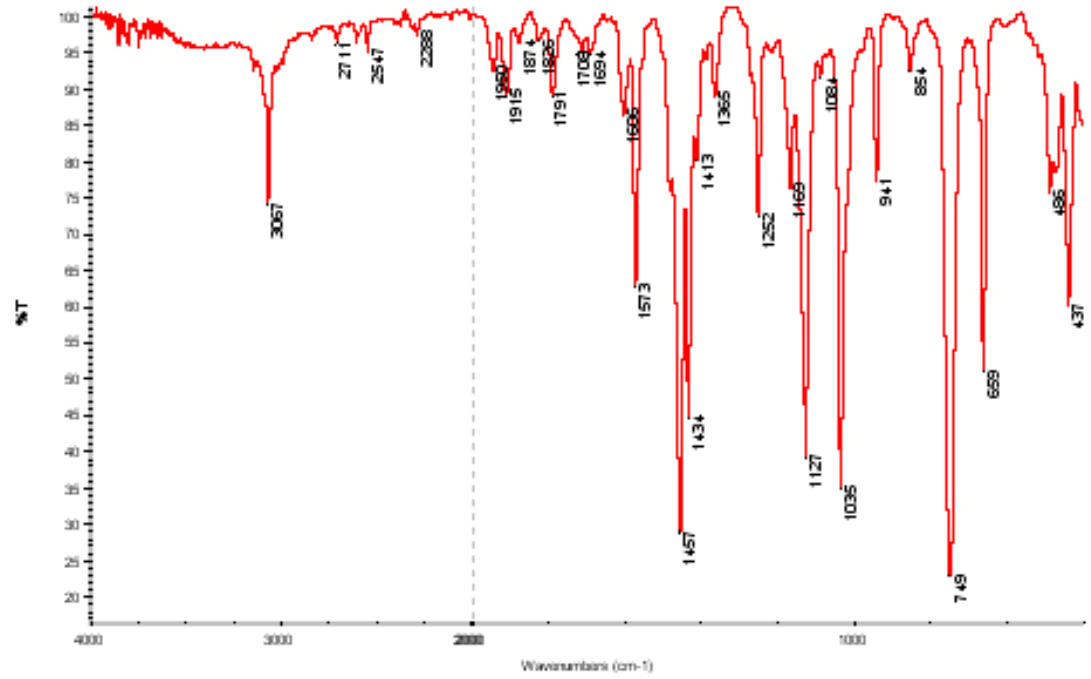

Fig. S4-7 The IR spectra of 1g

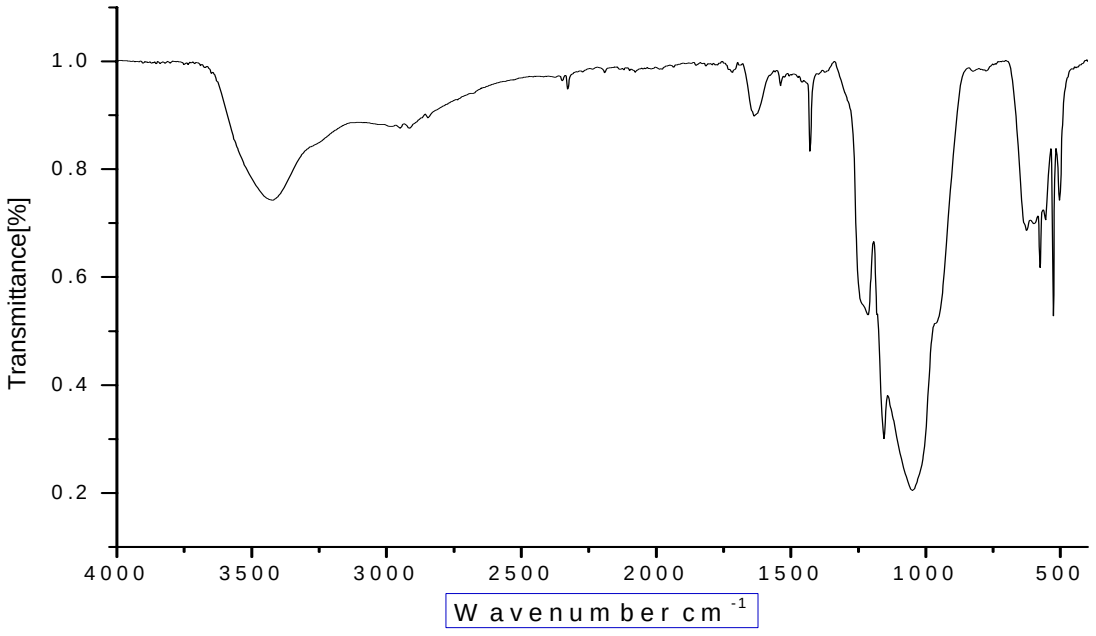

Fig. S4-8 The IR spectra of 2a

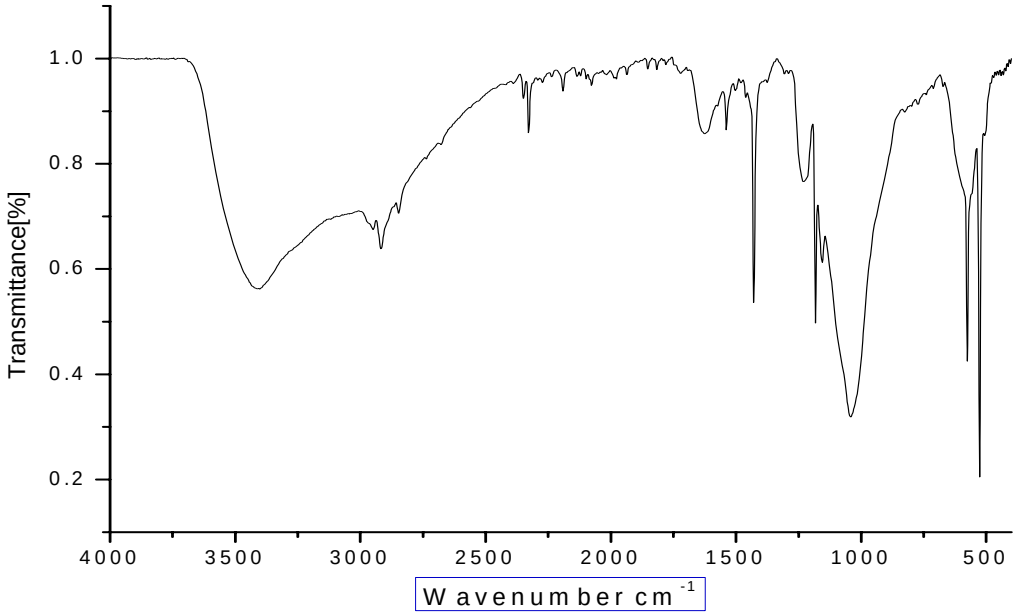

Fig. S4-9 The IR spectra of 2b

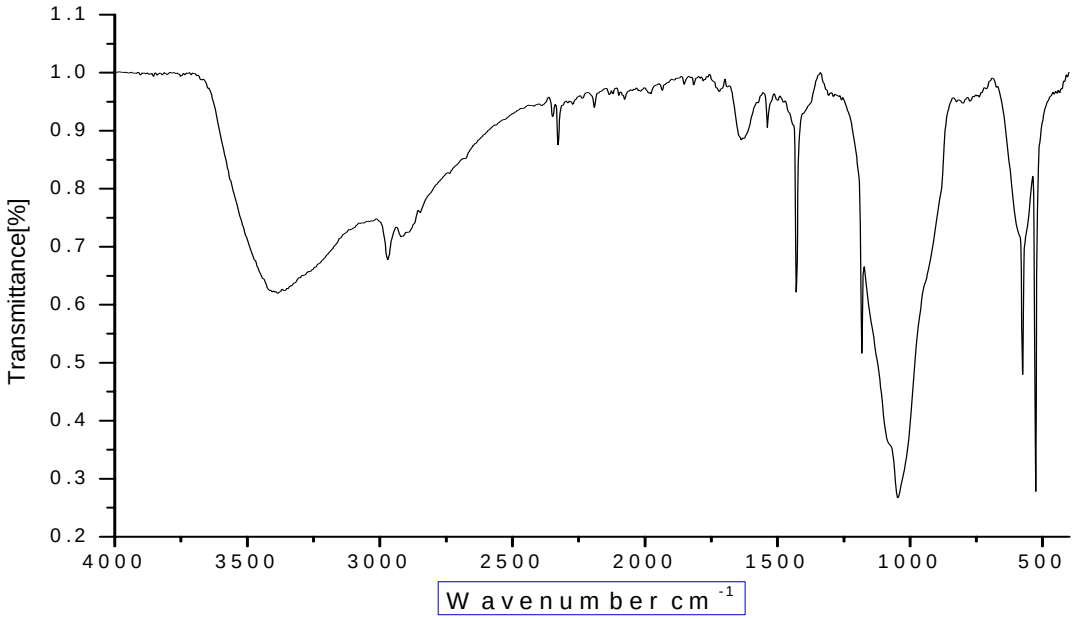

Fig. S4-10 The IR spectra of 2c

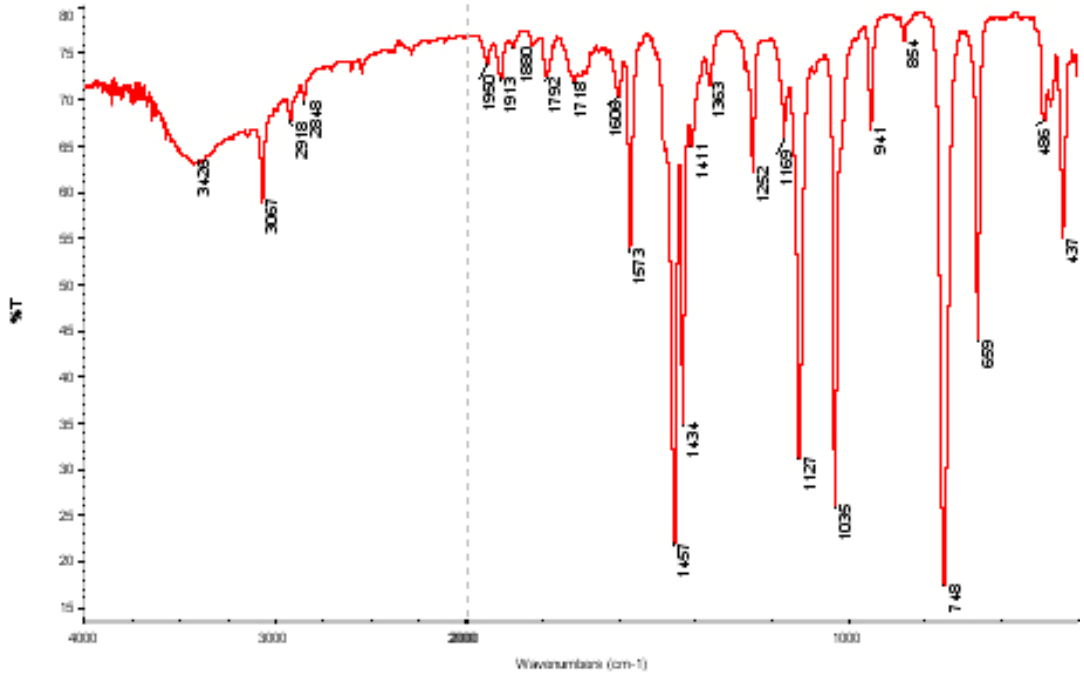

Fig. S4-11 The IR spectra of 2d

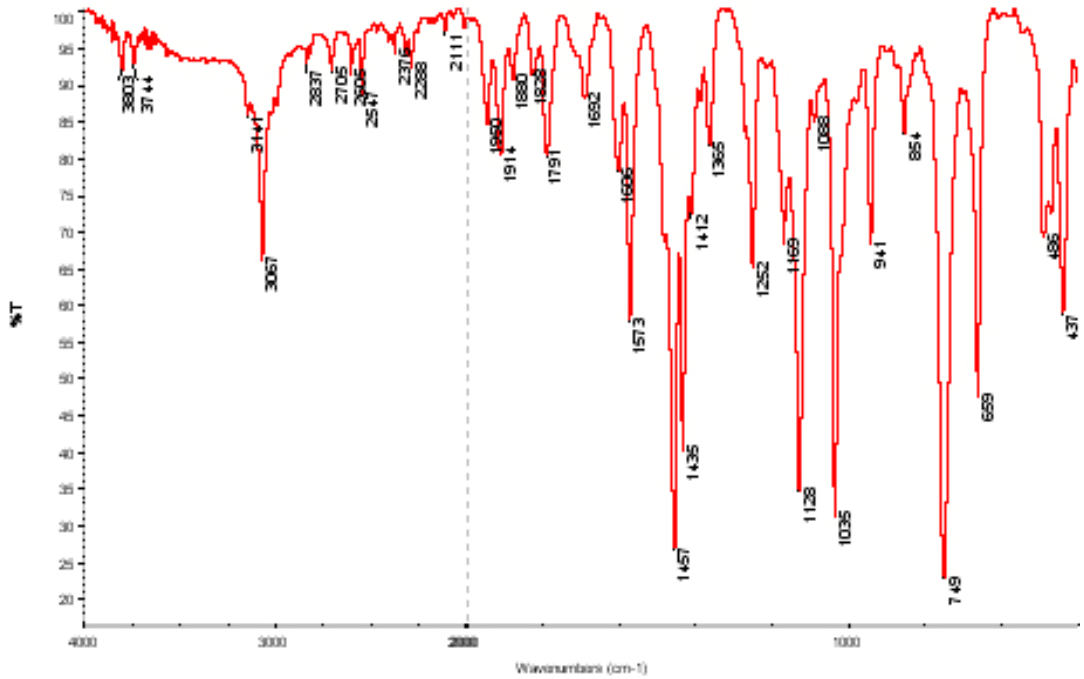

Fig. S4-12 The IR spectra of 2e

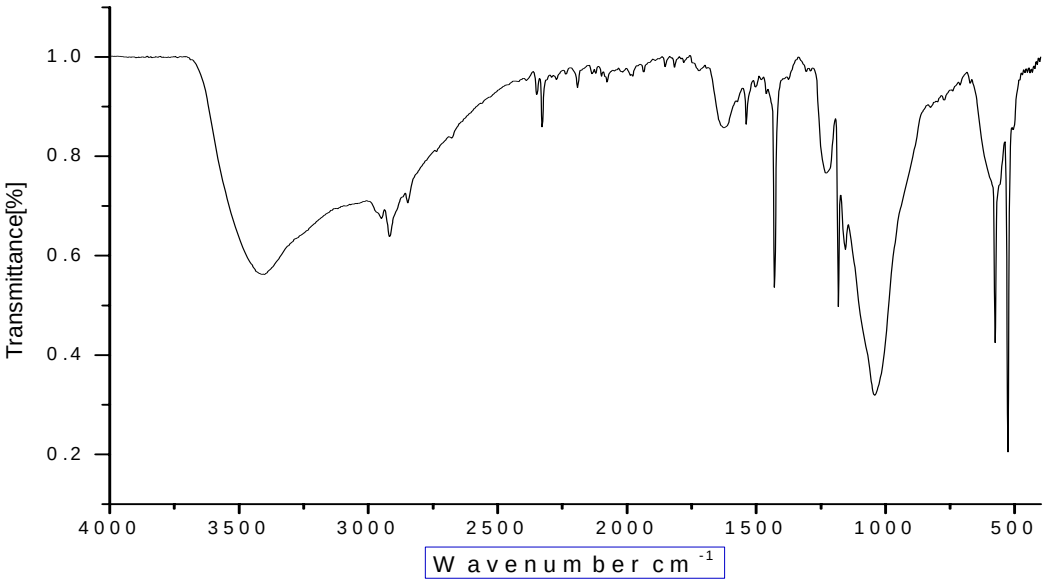

Fig. S4-13 The IR spectra of 2e

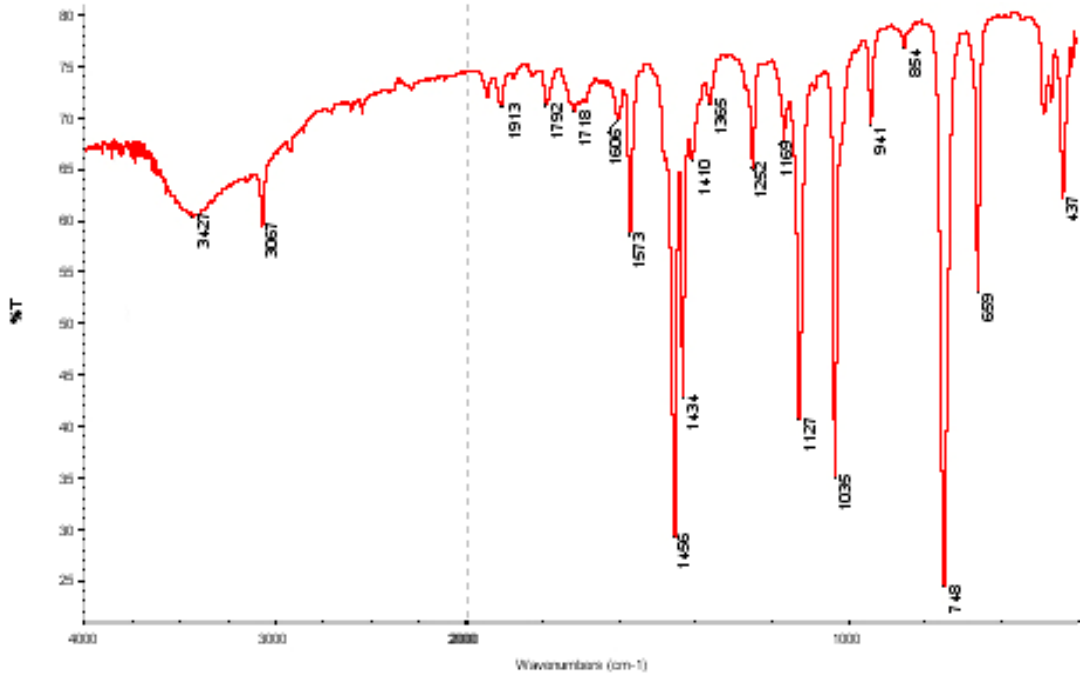

Fig. S4-14 The IR spectra of 2g

4. ^{1}H, ^{13}C, and ^{31}P NMR spectroscopy

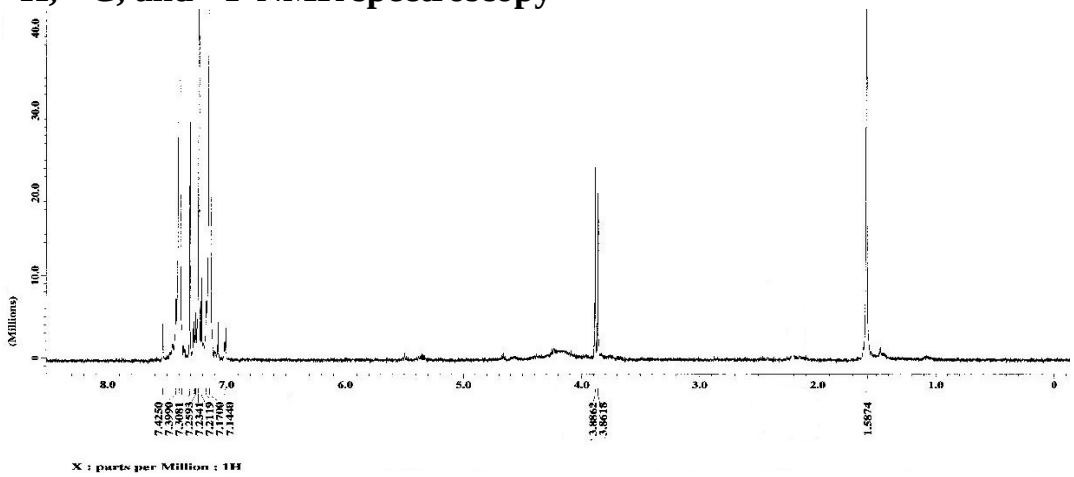

1d ^{1}H-NMR

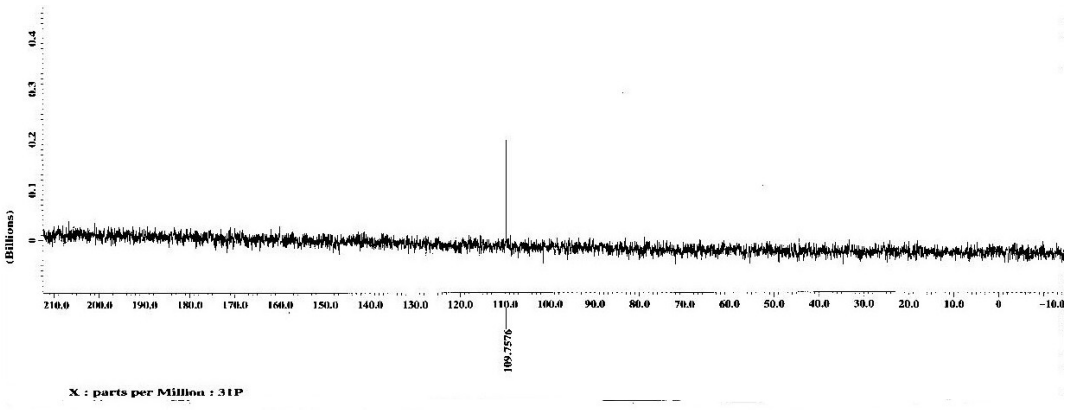

1d ^{31}P-NMR

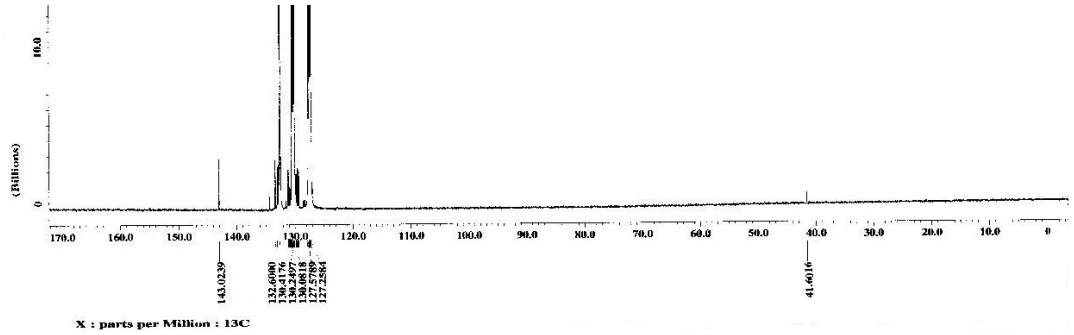

1d ^{13}C-NMR

Fig. S5-1 ^{1}H, ^{31}P and ^{13}C NMR spectroscopy of complexes **1d**

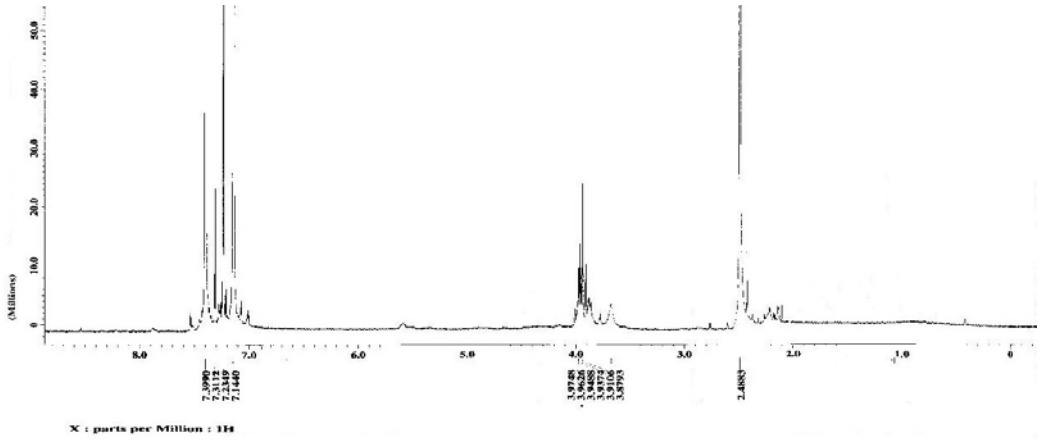

1g ^{1}H-NMR

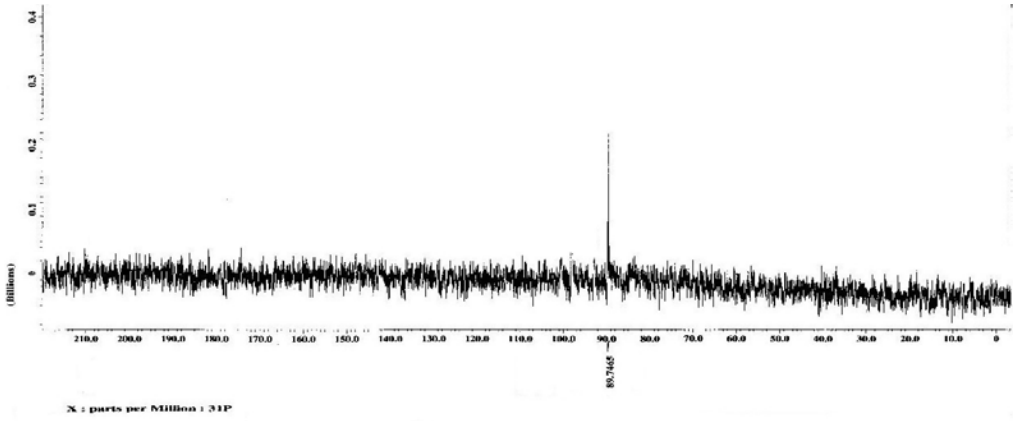

1g ^{31}P-NMR

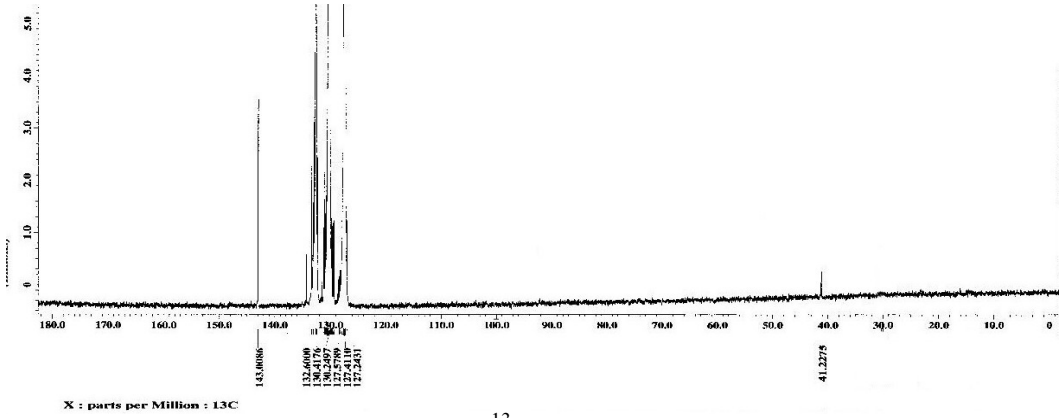

1g ^{13}C-NMR

Fig. S5-2 ^{1}H , ^{31}P and ^{13}C NMR spectroscopy of complexes **1g**

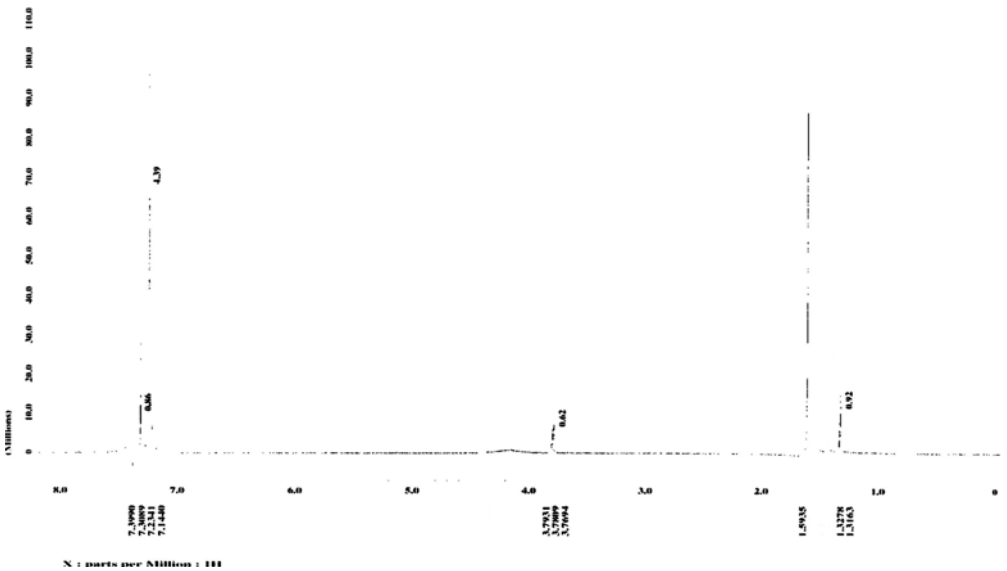

2d ^{1}H-NMR

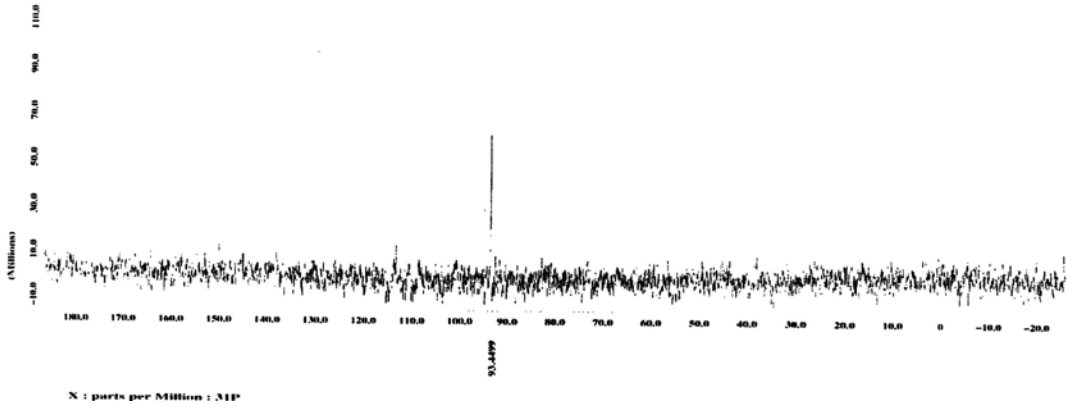

2d ^{31}P-NMR

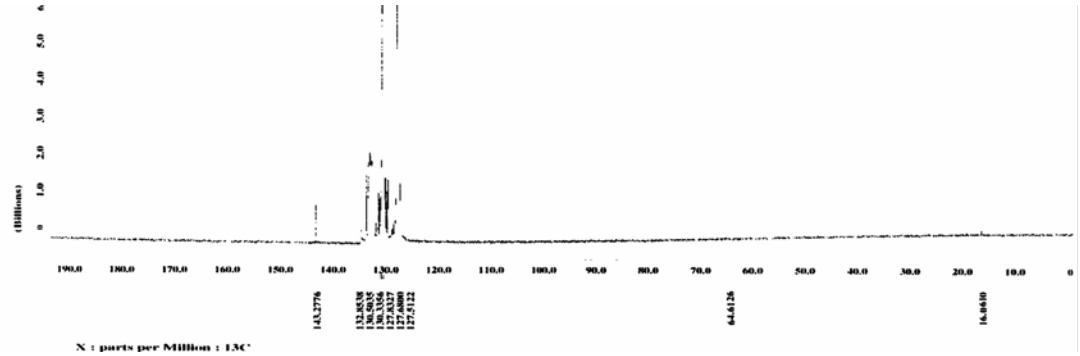

2d ^{13}C-NMR

Fig. S5-3 ^{1}H , ^{31}P and ^{13}C NMR spectroscopy of complexes **2d**

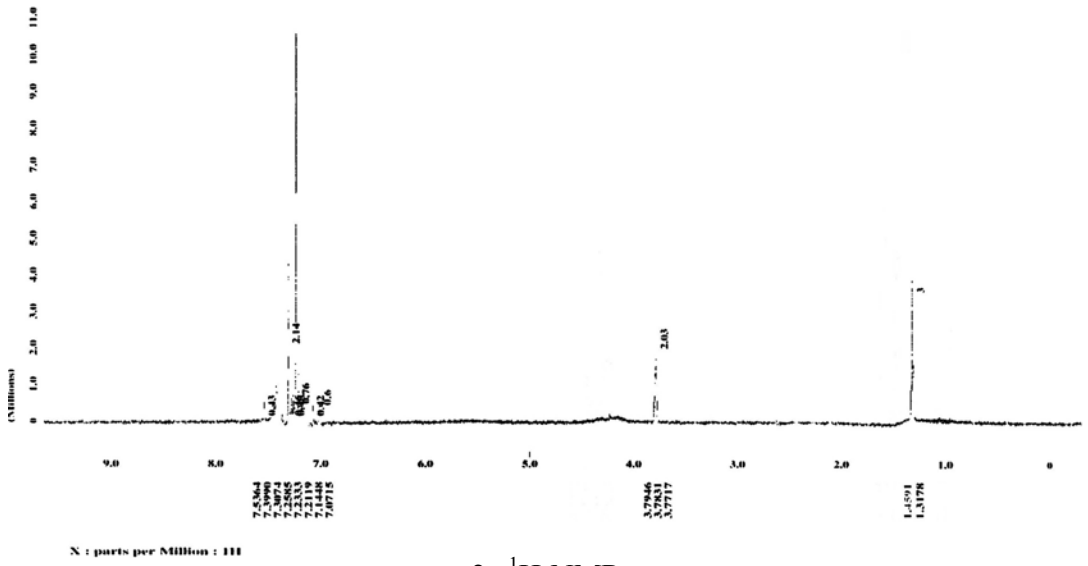

2e ^{1}H-NMR

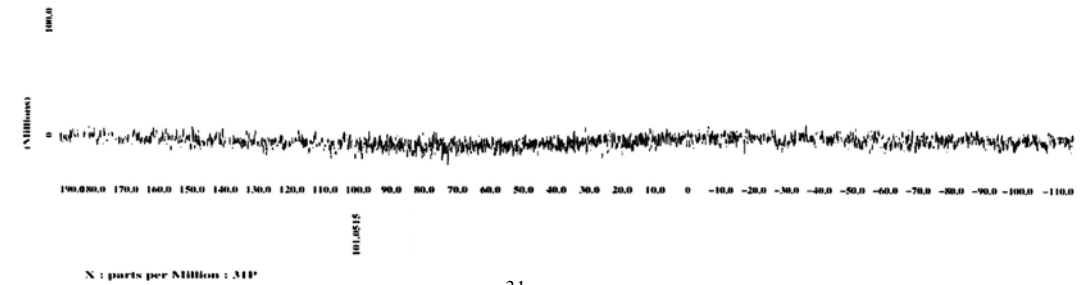

2e ^{31}P-NMR

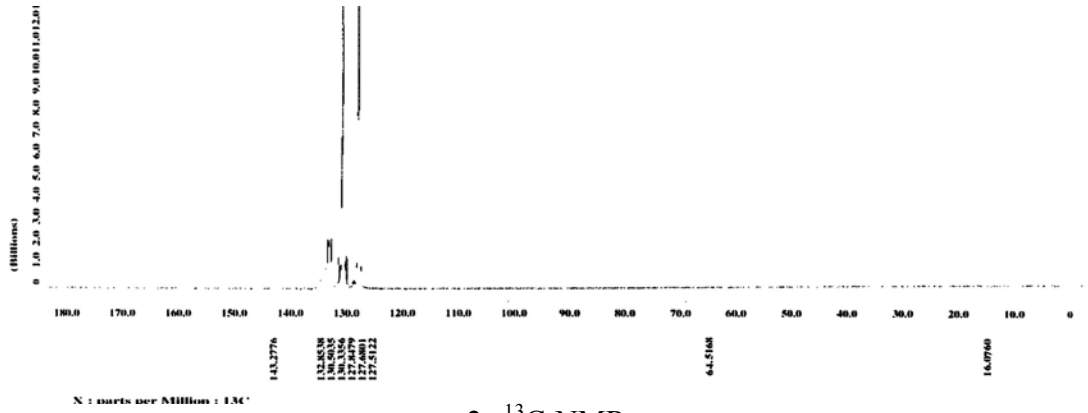

2e ^{13}C-NMR

Fig. S5-4 ^{1}H , ^{31}P and ^{13}C NMR spectroscopy of complexes **2e**

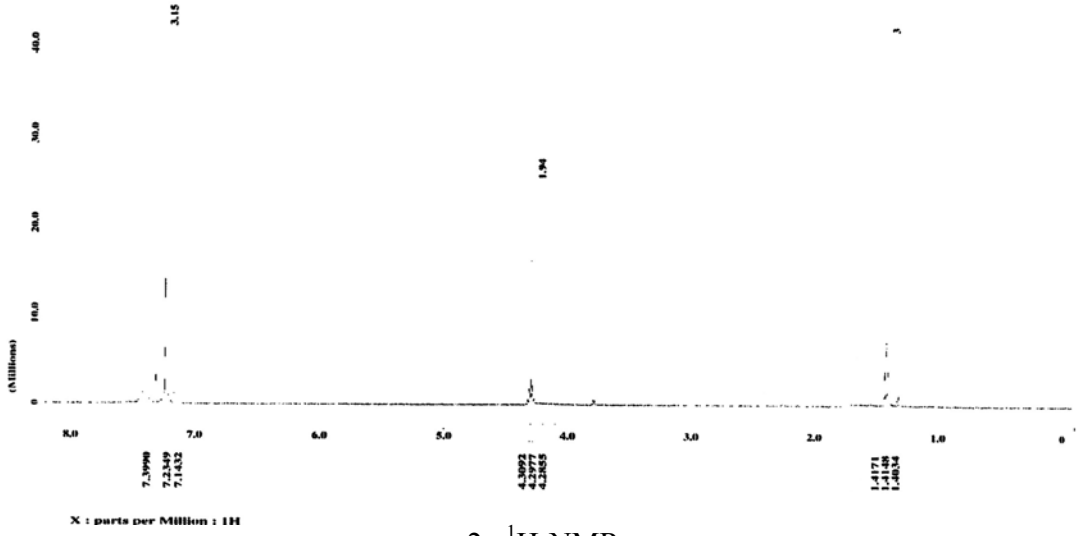

2g ^{1}H-NMR

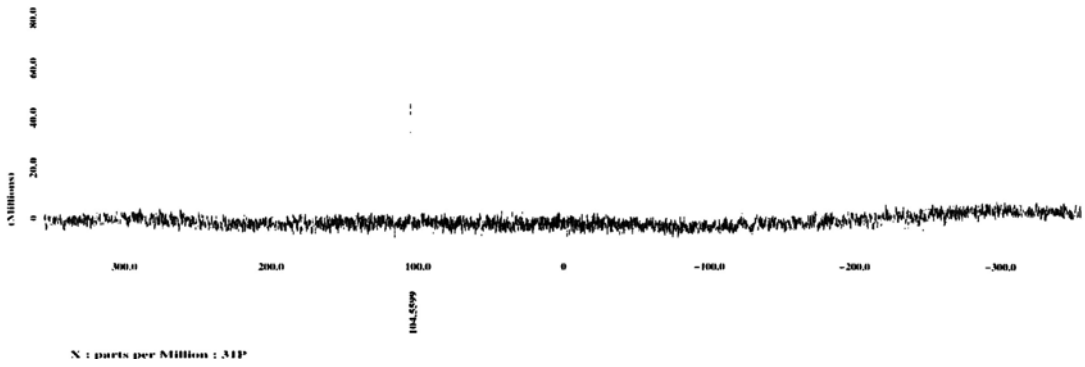

2g ^{31}P-NMR

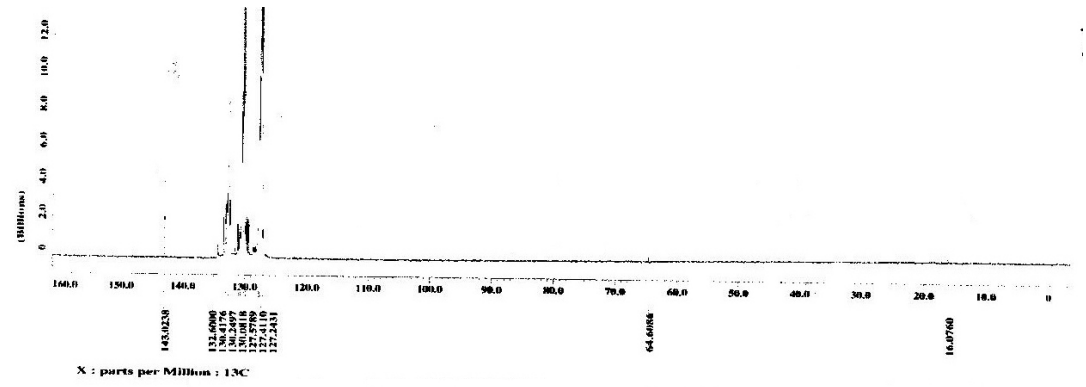

2g ^{13}C-NMR

Fig. S5-5 ^{1}H , ^{31}P and ^{13}C NMR spectroscopy of complexes **2g**

5. Open-aperture Z-scan data in *o*-dichlorobenzene solution

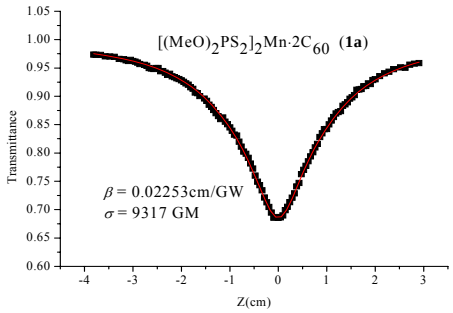

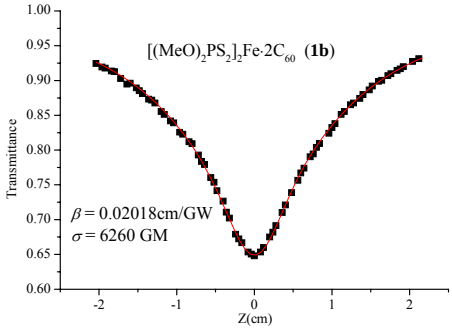

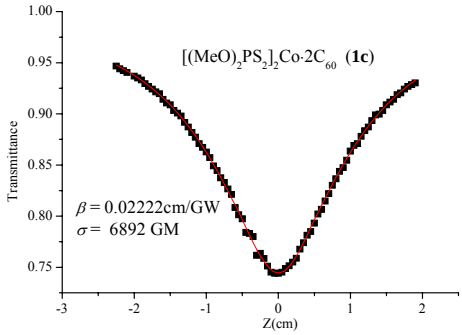

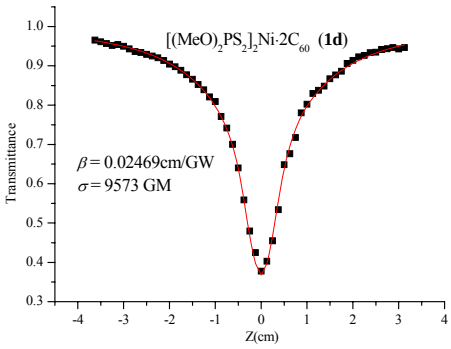

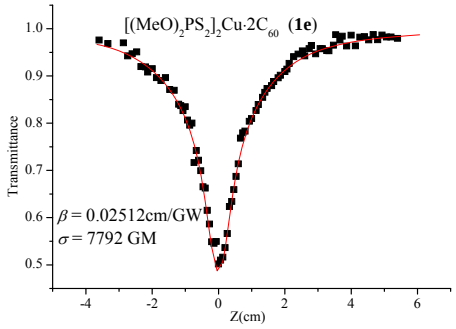

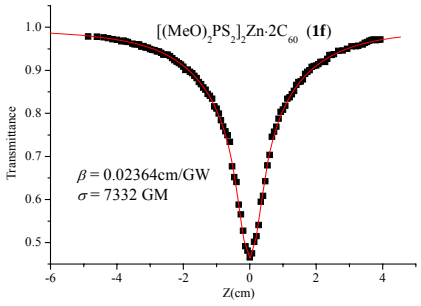

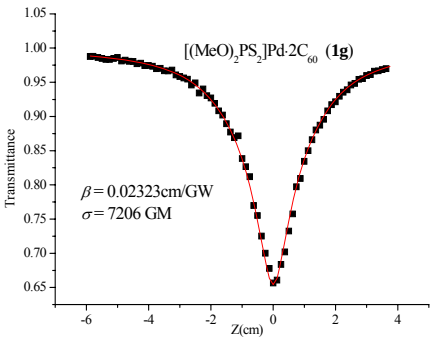

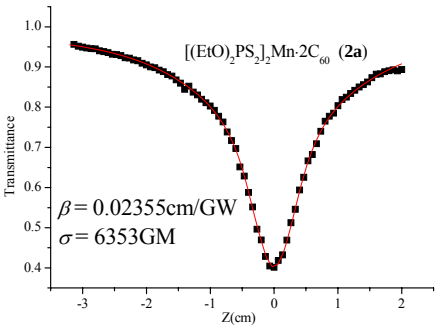

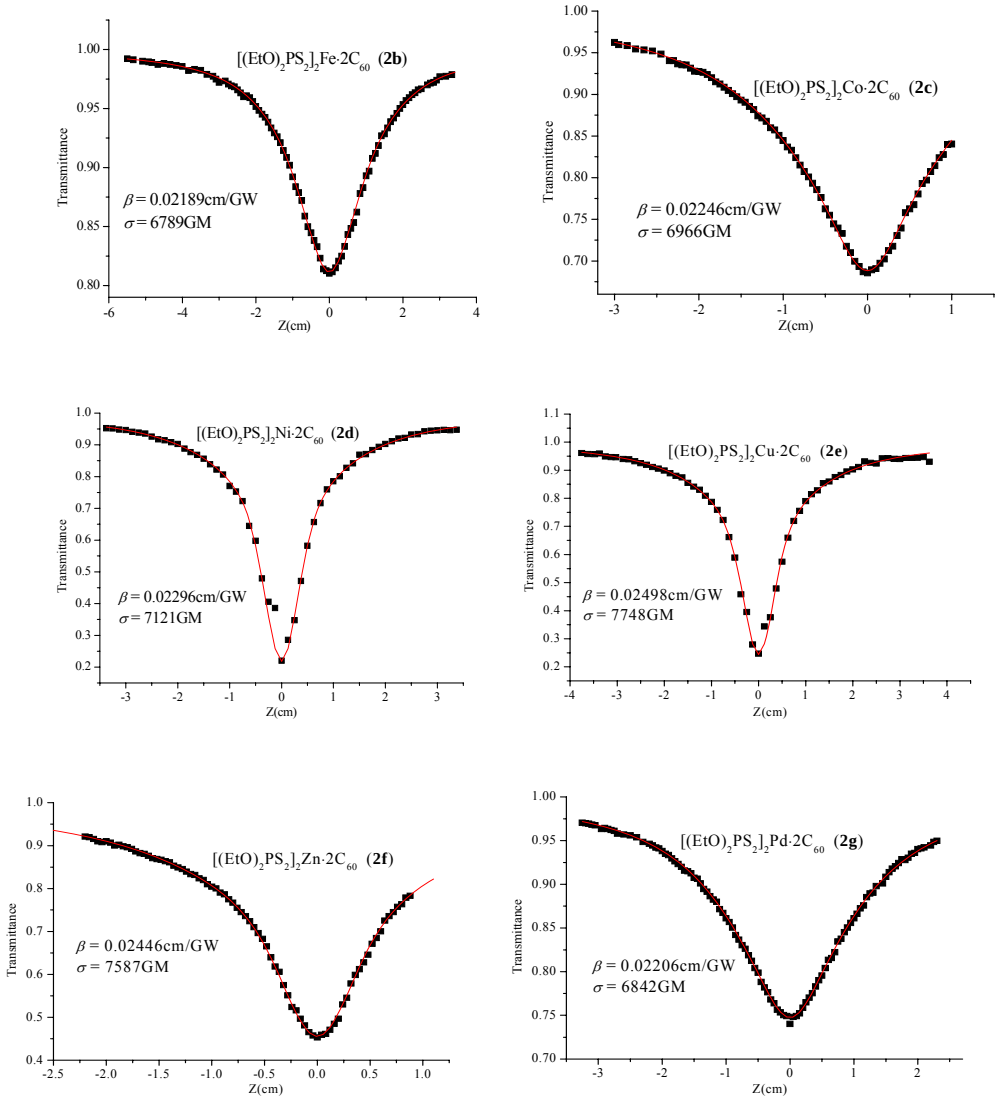

Fig. S6. Open-aperture Z-scan data in *o*-dichlorobenzene solution: normalized transmittance of the complexes of fullerene C_{60} with metal dialkyldithiophosphate. Scatter points are experimental data, and solid curves are theoretical fitting results.

6. Open-aperture Z-scan data in solid state

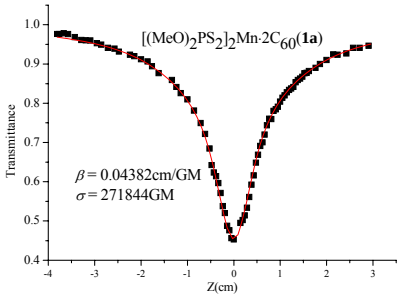

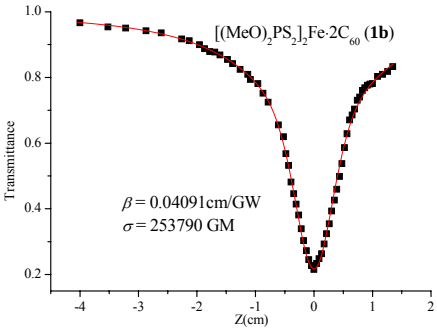

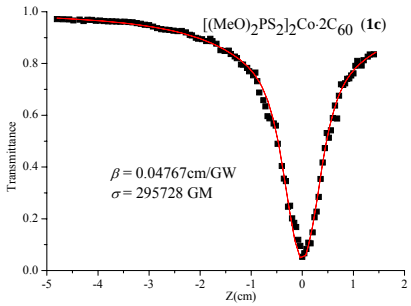

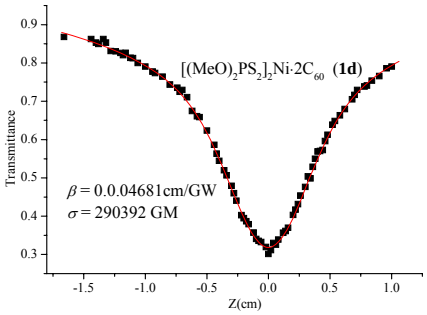

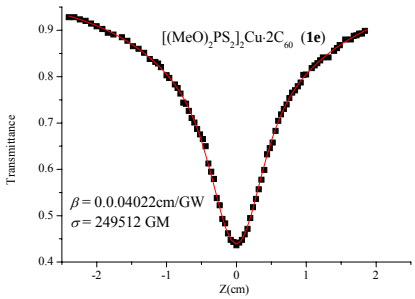

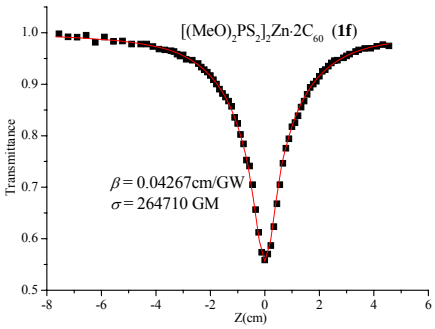

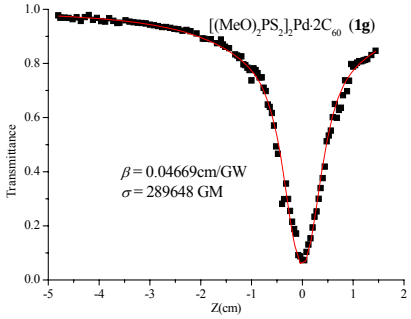

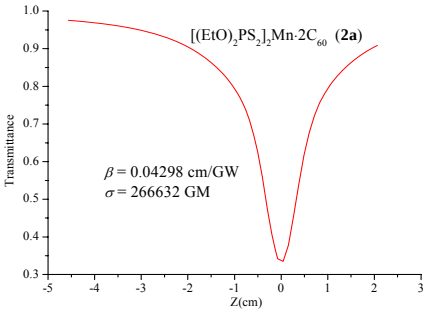

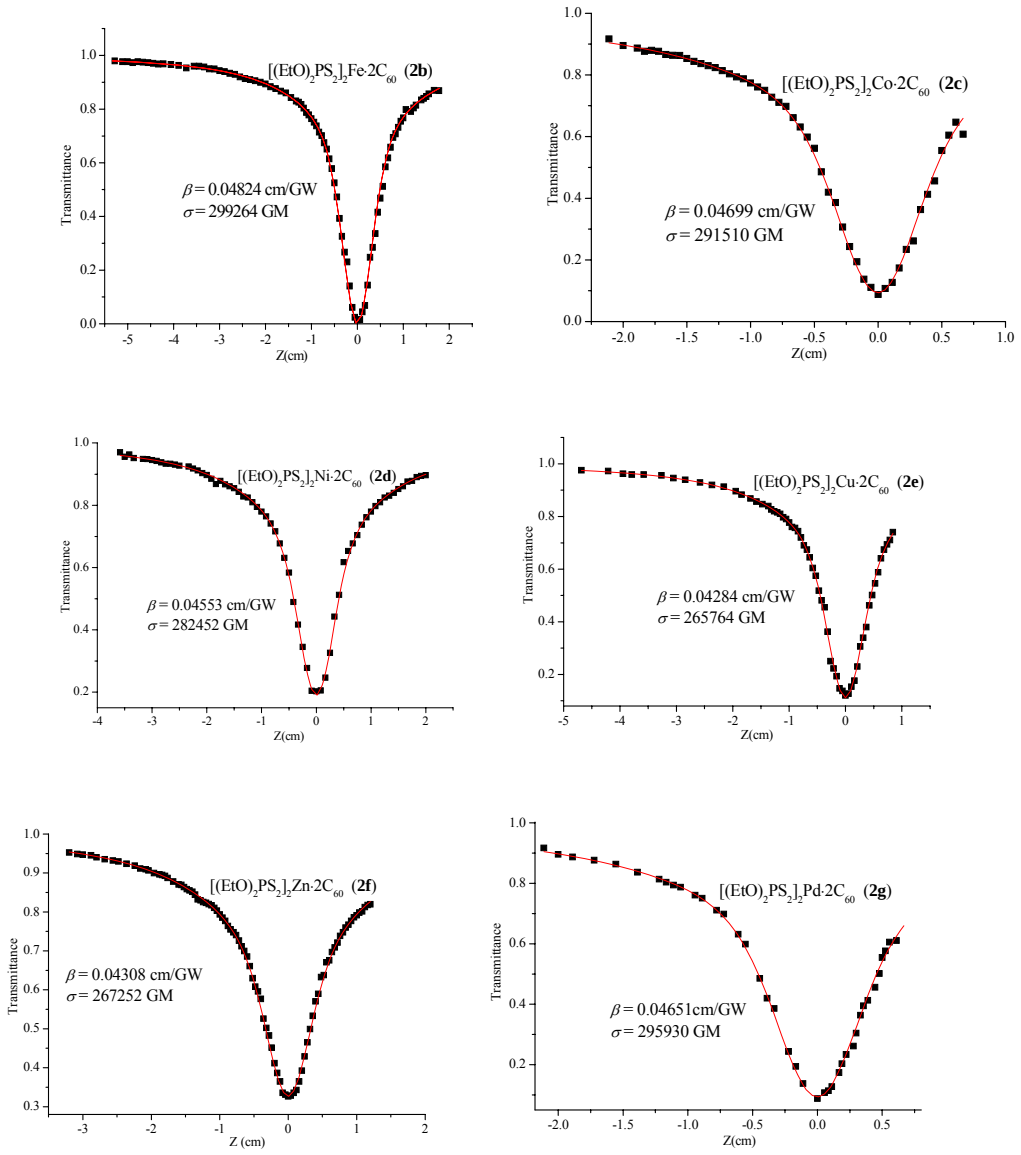

Fig. S7. Open-aperture Z-scan data in solid state: normalized transmittance of the complexes of fullerene C_{60} with metal dialkyldithiophosphate. Scatter points are experimental data, and solid curves are theoretical fitting results.

7. $[(CH_3O)_2PS_2]_2Ni{\cdot}2C_{60}$ 1d is calculated by density functional method at B3LYP/6-31G level of theory.

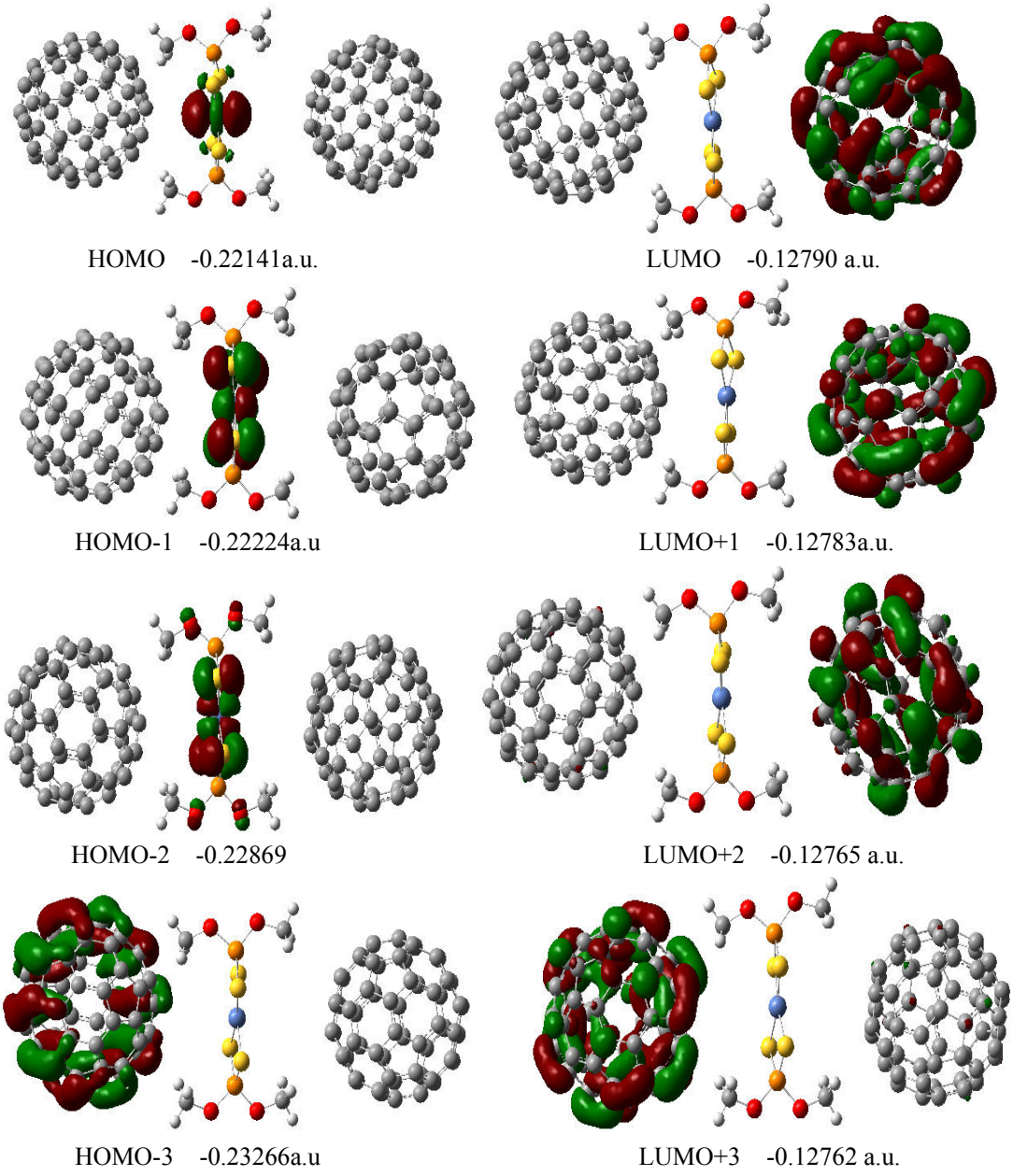

Fig. S8 The frontier molecular orbitals of **1d**